

Autotransporter Genes *pic* and *tsh* Are Associated with *Escherichia coli* Strains That Cause Acute Pyelonephritis and Are Expressed during Urinary Tract Infection

Susan R. Heimer,¹ David A. Rasko,² C. Virginia Lockett,³ David E. Johnson,^{3,4} and Harry L. T. Mobley^{1*}

Department of Microbiology and Immunology,¹ and Division of Infectious Diseases,³ University of Maryland School of Medicine, Baltimore, Maryland 21201; The Institute for Genomic Research, Rockville, Maryland 20850²; and Department of Veteran Affairs, Baltimore, Maryland 21201⁴

Received 1 July 2003/Returned for modification 5 August 2003/Accepted 22 September 2003

We have identified two chromosomal open reading frames in uropathogenic *Escherichia coli* (UPEC) strain CFT073 which are highly homologous to serine protease autotransporters Pic and Tsh. Both cloned determinants were correlated with the presence of 105- to 110-kDa proteins in the culture supernatants. Furthermore, in cellular fractionation experiments, 30-kDa polypeptides were identified in the outer membrane; we speculated that these proteins are the β -barrel portions of the autotransporter homologues. Furthermore, Pic-containing culture supernatants have serine protease activity. In reverse transcription-PCR analyses, the expression of the *pic* and *tsh* genes in *E. coli* CFT073 was higher in broth cultures grown at 37°C than at 25°C. Moreover, *pic* and *tsh* were expressed by bacteria isolated from urine of transurethral infected mice. The *tsh* determinant was identified in 63% of our clinical UPEC strain isolates ($n = 87$) and in 33% of fecal strains ($n = 27$), whereas *pic* was present in 31% of the pyelonephritis ($n = 67$) and 7% of the fecal strains. There was no significant correlation between cystitis strains ($n = 20$) and the *pic* determinant.

Uropathogenic *Escherichia coli* (UPEC) encodes a variety of genetic determinants that are associated with virulence. Guyer et al. have previously identified a novel secreted autotransporter toxin (Sat) in culture supernatants of strain CFT073 that is responsible for vacuolating cultured bladder and kidney epithelial cells (10, 11). Sat shares a high degree of homology with an expanding class of serine protease autotransporters in *E. coli* (SPATEs). In this study, we describe two additional SPATE proteins in CFT073 that are homologous to Pic and Tsh.

The Pic protein was originally identified in culture supernatants of enteroaggregative *E. coli* (EAEC) (12). Its genetic determinant overlaps with *shetAB*, which encodes the Shet1 enterotoxin (2, 12). This toxin is responsible for fluid accumulation in rabbit ileal loops (7). Like other SPATE proteins, Pic has been shown to have serine protease activity capable of acting on mucin (12).

Tsh was first reported as a temperature-sensitive hemagglutinating factor in avian pathogenic *E. coli* (APEC) (18). Its identical homologue, Hbp, was described as a heme-binding protein with a serine protease activity targeted at hemoglobin (16). Researchers have found that Hbp expression enhances abscess formation in mice during mixed infections with Hbp-expressing *E. coli* and *Bacteroides fragilis* (15).

We hypothesized that the CFT073 genes homologous to *pic* and *tsh* encode SPATE proteins which are secreted and proteolytically active. Moreover, we speculated that these deter-

minants are more prevalent among UPEC isolates than fecal strains.

Homology of CFT073 *pic* and *tsh* determinants. We identified the *pic* and *tsh* determinants while annotating the genomic sequence of *E. coli* CFT073 (gbAE014075) (22). The Pic homologue is well conserved (96% amino acid identity) among UPEC strain CFT073, EAEC strain 042, and *Shigella flexneri* 2a. This homology is evenly distributed across the protein, including the serine protease motif (GDSGSP), signal sequence, and β -barrel domains (12). As expected, *shetAB* homologues are present within the *pic*-coding region on the complementary strand (2). However, a transitional mutation in *shetA* (G to A at position 441) results in a premature stop codon 86 bp upstream from the expected 3' end. Thus, *shetA* may not be fully translated.

In comparison, the CFT073 Tsh homologue is slightly less conserved relative to its counterpart in APEC and the Hbp protein of intraabdominal *E. coli* (78% identity). Importantly, the β -barrel domain, serine protease motif, and amino acids flanking the predicted β -barrel cleavage site (residues 1109 to 1114) are identical among the Tsh homologues, whereas the signal sequences are considerably less conserved (30% identity) (16, 20).

Expression of CFT073 *pic* and *tsh* determinants. To circumvent any detection problems arising among the seven autotransporter homologues in strain CFT073, the *pic* and *tsh* determinants were separately PCR amplified from genomic DNA using the Expand Long Template PCR system with the following primer pairs: for *pic*, 5'-GCTAGCACGAGTATAATTAA TGGTGGCAG-3' and 5'-CTCGAGCGCATATACACACTC ACCAACTTG-3'; for *tsh*, 5'-GCTAGCAGATGATGGTAT GGTGAT-3' and 5'-CTCGAGTTCAGCCTGTACCGTAA

* Corresponding author. Mailing address: Department of Microbiology and Immunology, University of Maryland School of Medicine, 655 W. Baltimore St., Baltimore, Maryland 21201-1192. Phone: (410) 706-0466. Fax: (410) 706-6751. E-mail: hmobley@umaryland.edu.

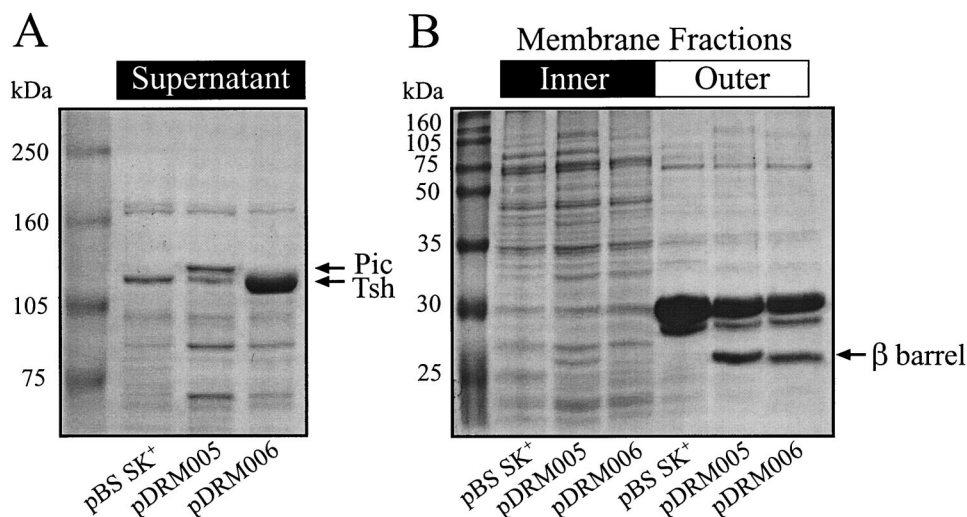


FIG. 1. Expression of autotransporter proteins from cloned *pic* and *tsh* determinants. Concentrated culture supernatants (A) and membrane fractions (B) prepared from *E. coli* BL21(DE3) pLysS transformed with either pBS SK⁺, pDRM005 (*pic*), or pDRM006 (*tsh*) were separated in SDS-10% (A) or -12% (B) PAGE and stained with Coomassie blue. The relative migrations of molecular mass standards are indicated at the left. Arrows denote protein bands that correspond to the predicted electrophoretic mobilities of Pic and Tsh proteins.

TCAG-3'. Subsequently, products were cloned into pBS KS⁺ under T7 promoter control. *E. coli* BL21(DE3) pLysS (*ompT*) pDRM005 (*pic*) or pDRM006 (*tsh*) transformants were cultured overnight at 37°C in 100 ml of agitated L broth supplemented with ampicillin (25 µg/ml) and chloramphenicol (10 µg/ml) (8). Sterile bacterial supernatants were concentrated with a Centricon Plus-80 spin filter (100-kDa cutoff). As predicted, a distinct 115-kDa protein band was observed in the concentrated supernatant of pDRM005 (*pic*) transformants in a sodium dodecyl sulfate-polyacrylamide gel electrophoresis (SDS-PAGE) analysis (Fig. 1A, lane 3). This band was absent from the vector control (lane 2). Likewise, a 110-kDa protein band was noted in the supernatant of pDRM006 transformants as expected of mature Tsh protein (Fig. 1A, lane 4); however, an analogous protein was also seen in the vector control (lane 2). Given the relative abundance of these proteins, we speculated that *tsh* is expressed in the pDRM006 strain (lane 4) and comigrates with a protein secreted by the host strain.

To establish whether the conserved β -barrel domains localize to the outer membrane, both inner and outer membrane fractions were prepared from bacterial lysates (10). In SDS-PAGE analysis, protein bands (27 kDa) were seen in outer membrane fractions of both pDRM005 and pDRM006 transformants (Fig. 1B, lane 6 [*pic*] and lane 7 [*tsh*], respectively) that were absent from the vector control (lane 5). These protein bands were similar to the predicted sizes of both Pic and Tsh β -barrel domains (30 kDa). There are many examples of mature autotransporter proteins that are cleaved away from the β -barrel domains upon secretion (13). Although we do not provide direct evidence, these data are consistent with a similar processing of Pic and Tsh in the host strain BL21(DE3) (*ompT*). On occasion, we have observed full-length Pic and Tsh proteins to copurify with membrane fractions (data not shown). We postulate that those products are tethered to the outer membrane via the β -barrel at the C terminus.

Proteolytic activity of the Pic protein. To determine if the secreted proteins had serine protease activity, concentrated culture supernatants (2.0 µg of total protein) were incubated with casein conjugated to Bodipy FL (5 µg) overnight at 37°C (10). As seen in Fig. 2, both Pic- and Sat-containing supernatants were capable of hydrolyzing casein. Note Sat is also a SPATE protein as previously described (10). Furthermore, no activity was detected in the presence of a serine protease inhibitor, phenylmethylsulfonyl fluoride (PMSF) (Fig. 2). In contrast, Tsh-containing supernatants behaved similarly to the

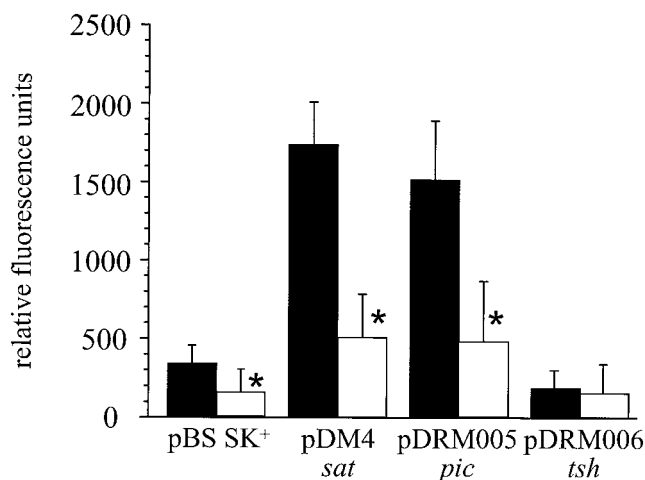


FIG. 2. Protease activity of culture supernatants. Concentrated culture supernatants (2 µg) were incubated with a casein-Bodipy FL derivative (5 µg) at 37°C for 20 h in the absence (black bars) or presence (white bars) of 500 µM PMSF. Relative fluorescence units were measured at 535 nm using an excitation wavelength of 485 nm. Data represent triplicate measurements of three independent experiments. Asterisks denote significant differences in mean values of samples lacking and containing PMSF (unpaired *t* test, $P < 0.005$).

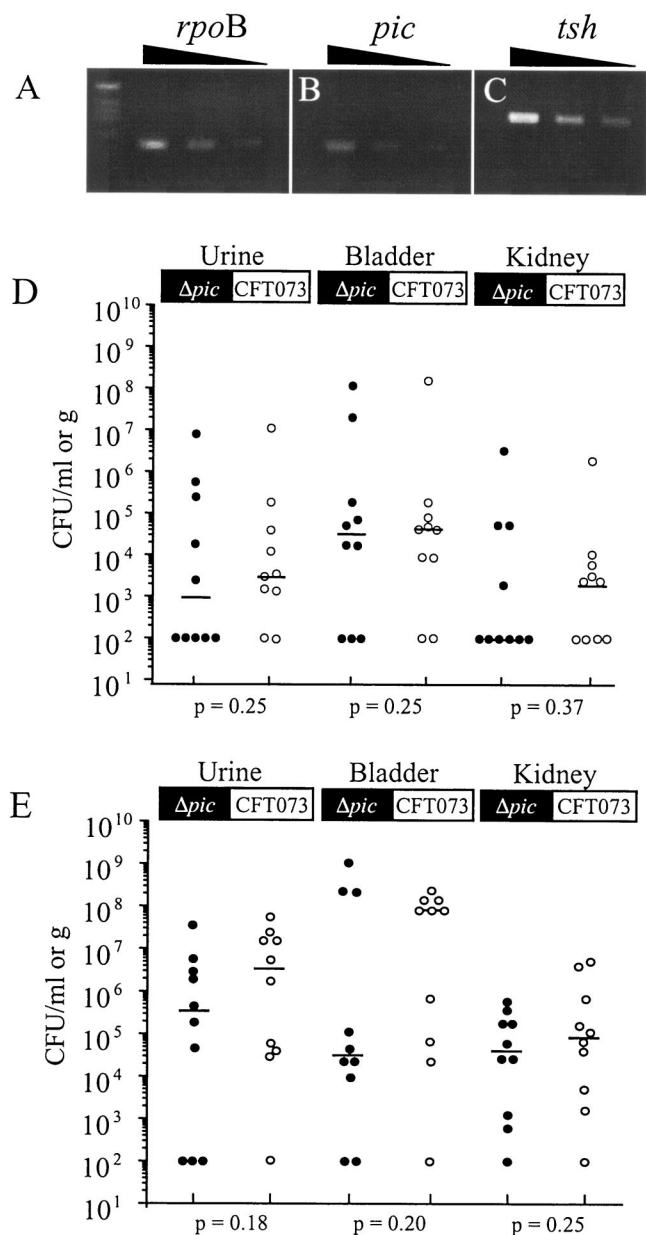


FIG. 3. CBA mouse model of ascending UTI. (A to C) Ten female CBA mice were challenged transurethraly with CFT073 ($\sim 1.0 \times 10^9$ CFU). Twenty-four hours postinoculation, tissue and urine samples were collected, homogenized, and quantitatively cultured on L agar. A median value of 1.8×10^6 CFU/ml of urine was isolated from infected animals, whereas only 90 CFU/ml of urine was obtained from uninfected animals. Bacteria isolated from pooled urine samples ($n = 10$) were analyzed by RT-PCR using three gene-specific primer pairs. Serially diluted RT-PCR products were separated in 2.0% agarose gel. (D) Female CBA mice were cochallenged transurethraly with CFT073 and CFT073 Δpic (1:1) with 1.0×10^9 CFU per animal ($n = 10$). Six days postinoculation, tissue and urine samples were collected from each animal. Homogenized tissue and urine samples were quantitatively cultured on L agar. Values are the CFU per milliliter of urine or gram of tissue along with the median value of each group (horizontal line). (E) In a similar experiment, mice were independently challenged with CFT073 or CFT073 Δpic with 1.0×10^9 CFU per animal ($n = 10$). Statistical differences between wild-type and mutant strains were determined by a one-tailed Wilcoxon matched pairs test (D) or Mann-Whitney test (E).

vector control strain. Analogous results were observed with an elastase IV substrate-pNA conjugate (500 μ M) using 5 μ g of supernatants (20 h; 37°C) (data not shown). Concentrated EAEC Pic and APEC Tsh preparations were used as positive controls (6). From these results, it can be concluded that secreted Pic has serine protease activity. Unfortunately, we have had no success identifying a mucinase activity associated with CFT073 Pic (data not shown) or the EAEC homologue which has been reported elsewhere (12). Likewise, preliminary experiments in heme-binding and hemoglobinase activity with CFT073 Tsh have also been inconclusive (16, 21).

CFT073 expression of *pic* and *tsh* is upregulated at 37°C. To confirm the expression of *pic* and *tsh* in their native background, cDNA was prepared from CFT073 cultures and PCR amplified with internal gene-specific primers. Bacterial cells (5×10^8) were collected during logarithmic-phase growth in L broth at 25 or 37°C and flash-frozen for storage. Subsequently, DNA-free RNA was isolated from thawed bacterial cells with RNeasy mini columns. cDNA was synthesized using a randomly primed Superscript First Strand system and digested with RNase H. As a negative control, synthesis reactions were also prepared without Superscript II reverse transcriptase. To identify cDNAs encoding *rpoB*, *pic*, and *tsh*, internal regions within each determinant were PCR amplified with the following primer pairs: for *rpoB* (145bp), 5'-CACCGTGACATCCCGAACG-3' and 5'-ATCGCACGCAGCAGTTTTTC-3'; for *pic* (120 bp), 5'-AACGGACCTTTACCTGACTA-3' and 5'-TTCCACCAGTTCGTAGCACC-3'; for *tsh* (269 bp), 5'-GTCAGGTCAGTAACGAGCAC-3' and 5'-AGAGACGAGACTGTATTTGC-3'.

Reverse transcription-PCR (RT-PCR) products were observed with *pic*- and *tsh*-specific primers at 120 and 269 bp, respectively. These products were absent in reactions not containing reverse transcriptase (data not shown). Interestingly, the relative amounts of *pic* and *tsh* RT-PCR products differed between cultures grown at 25 and 37°C. By comparing band intensities, we calculated a 4.1-fold increase ($n = 10$) in *pic* products at 37°C and, correspondingly, a 2.3-fold increase ($n = 12$) in *tsh* products. On the other hand, comparable quantities of *rpoB* products (145 bp) were detectable in 25 and 37°C cultures (1.1-fold; $n = 12$). If we assume that the relative quantity of RT-PCR products can be correlated with the amount of isolated mRNA, then *pic* and *tsh* expression was significantly enhanced at 37°C compared to *rpoB* expression (t test; $P = 0.002$ and $P = 0.0007$, respectively).

Other researchers have reported increased protein concentrations of Pic and Tsh in culture supernatants when cells were grown in rich medium at 37°C compared to 25°C (12, 20). Moreover, the processing of pro-Hbp was shown to be impaired at 26°C, which contributed to reduced extracellular concentrations (16). In CFT073, the transcriptional regulation of *pic* and *tsh* appears to be temperature sensitive. Interestingly, in EAEC, *pic* transcription appears to be growth phase dependent, favoring expression during early to mid-logarithmic phase (3). Both temperature- and growth phase-dependent expression could be key mechanisms for regulating virulence determinants during the early phases of infection among pathogenic strains.

CFT073 *pic* and *tsh* determinants expressed during infection. To establish whether *pic* and *tsh* determinants were expressed during infection, 10 female CBA/J/Hsd mice were in-

TABLE 1. Distribution of *pic* and *tsh* determinants among uropathogenic and fecal *E. coli* isolates

Source of <i>E. coli</i>	<i>n</i>	No. (%) of strains hybridizing with probe specific for:					
		<i>pic</i>		<i>tsh</i>		Both <i>pic</i> and <i>tsh</i> ^b	
		No. (%) of strains	<i>P</i> value ^a	No. (%) of strains	<i>P</i> value ^a	No. (%) of strains	<i>P</i> value ^a
Fecal	27	2 (7)		9 (33)		1 (4)	
Cystitis	20	3 (15)	0.350	13 (65)	0.031	3 (15)	0.200
Pyelonephritis	67	21 (31)	0.011	42 (61)	0.009	17 (25)	0.011

^a Statistical significance between fecal and cystitis (or pyelonephritis) distributions was determined with a one-tailed Fisher's test for exactness.

^b A total of 19% of pyelonephritis strains were positive for *sat*, *pic*, and *tsh*, whereas no fecal strains were positive for all three autotransporter genes.

oculated transurethrally with 10^9 CFU (50 μ l) via catheter (14). To assay for *rpoB*, *pic*, and *tsh* expression, bacteria were isolated from urine 24 h postchallenge and flash-frozen. Thawed samples were processed for RT-PCR analysis. For comparison, urine samples were also collected from 10 uninfected animals.

The bacterial counts of the pooled urine samples ranged from 1.8×10^6 CFU/ml (infected) to 90 CFU/ml (uninfected). Bacteria were also noted in the bladder (median value of 4.1×10^7 CFU/g) and kidneys (median value of 4.0×10^5 CFU/g) of infected animals. RT-PCR products corresponding to *pic*, *tsh*, and *rpoB* expression were detected in urine samples from infected animals (Fig. 3A, B, and C, respectively), whereas no products were observed with urine from uninfected animals (data not shown). We speculate that these conditions also reflect *pic* and *tsh* expression in the bladder.

Prevalence of *pic* and *tsh* determinants among UPEC isolates. To determine whether the *pic* and *tsh* determinants were preferentially associated with UPEC, we prepared dot blots with 87 *E. coli* isolates from patients diagnosed with acute pyelonephritis or exhibiting symptoms of cystitis (9, 19) and 27 *E. coli* fecal isolates from healthy women (9, 19). Internal probes of the *pic* and *tsh* determinants (see above) were created by PCR amplification in the presence of digoxigenin-labeled dUTP and detected with the digoxigenin luminescence detection system. Probe specificity was confirmed with dot blots of denatured plasmid preparations, including pPic, pAY3108, pDG7, pCEN1, pZK15, pB9-5, pJLM174, and pBS SK⁺, which encode the following SPATEs: *pic*, *tsh*, *sat*, *pet*, *sepA*, *espP*, *espC*, and vector control, respectively (data not shown) (10).

As described in Table 1, the *pic* probe hybridized to 21 of 67 (31%) of pyelonephritis isolates compared to only 2 of 27 (7%) fecal isolates. However, only 3 of 20 (15%) cystitis isolates were found to be *pic* positive. Based on these data, we propose that *pic* is preferentially encoded in pyelonephritis strains compared to fecal isolates (Fisher's exact test, one-tailed; $P = 0.011$) but is not necessarily associated with cystitis strains ($P = 0.35$). It is unclear whether these results reflect a particular role for *pic* in uropathogenesis or simply sample size. Analogous distributions of *pic* have been reported among clinical isolates of EAEC (39.7%) and *Shigella* spp. (27.7%) (1, 17).

In contrast, the *tsh* determinant was present in 42 of 67 (61%) pyelonephritis isolates and 13 of 20 (65%) cystitis isolates. The prevalence of *tsh* among fecal isolates (33%) was significantly lower than among the uropathogenic isolates ($n = 87$; Fisher's exact test, one-tailed; $P = 0.006$). These findings suggest that *tsh* is more frequently distributed among *E. coli*

associated with urinary tract infection (UTI) than commensal *E. coli*. These results agree with the distribution of the *tsh* homologue (*hbp*) among human extraintestinal (31%) and fecal (5%) isolates reported by Otto et al. (16). In a larger epidemiological study of APEC ($n = 253$), *tsh* was found in 39% of strains associated with colisepticemia versus only 3.8% in fecal strains (5).

Virulence assessment of a *pic* mutant in a CBA mouse model of ascending UTI. Based on the mucinase activity of the Pic homologue in EAEC (20) and the prevalence of *pic* among pyelonephritis strains, we speculated that the serine protease function of Pic might enhance *E. coli* CFT073 colonization and pathology in the urinary tract. To test this hypothesis, the *pic* determinant in CFT073 was replaced with a PCR product encoding *pic::cat* by homologous recombination mediated by the λ Red recombinase system (4). The *cat* PCR product was created with primer pairs 5'-AAGCAAACGAAAAGTATTTCACTATGTAACAGACATCACAGTGTAGGCTGGAGCTGCTTC-3' and 5'-TCATGGCTCATAACAGAACTACCATAAGAAGGATGATTAAGCATATGAATATCCCCCTTAGT-3'. Replacement recombination was confirmed by PCR amplification using primers that recognize *pic* flanking sequence (described above) and internally primed RT-PCR. Note that this mutation also eliminates *shetAB* encoded by the complementary strand. The morphology and growth rate of CFT073 Δ *pic* was not significantly altered compared to that of the wild-type strain. Furthermore, in L broth cocultures CFT073 Δ *pic* consistently maintained cell densities similar to the wild-type strain over 24 h at 37°C (data not shown).

Having confirmed competitive growth in vitro, 10 CBA mice were cochallenged transurethrally with CFT073 Δ *pic* and CFT073 using 10^9 CFU (1:1 mixture). Six days postinoculation, samples of the kidney, bladder, and urine were collected and quantitatively cultured on L agar. No significant differences were found between CFT073 Δ *pic* and wild-type colonization as indicated by the median numbers of CFU recovered per milliliter of urine or gram of tissue (Fig. 3D). Thus, we conclude that there was no competitive advantage of Pic-encoding strains in mixed infections. However, it is unclear whether wild-type protein secretion can complement a *pic*-deficient strain. Similar arguments can be made for the *shetAB* determinants of CFT073.

To study the relative pathologies caused by these organisms and avoid complementation by the wild-type strain, independent CBA mouse challenges were performed under similar conditions (Fig. 3E). The wild-type strain appeared to colonize the bladder to a greater extent (median value, 8.2×10^7 CFU/g) than CFT073 Δ *pic* (median value, 3.3×10^4 CFU/g); however, this trend was not statistically significant (Mann-Whitney test [one-tailed], $P = 0.20$). Likewise, histological

examination of the tissues suggested that these organisms produced similar pathology. However, there were subtle differences in the bladder pathologies of animals colonized with fewer than 1.0×10^8 CFU/gm of tissue. Under these conditions, four of six CFT073 infections displayed neutrophils infiltrating the lumen, epithelium, and submucosa, whereas neutrophils were found only in the lumen among one of five CFT074 Δ pic infections.

In conclusion, CFT073 encodes three SPATE homologues, *sat*, *pic*, and *tsh*. These determinants have been found more frequently in UPEC strains than fecal *E. coli*, suggesting a role in virulence. Animal experiments indicate that the role of Sat and Pic in CFT073 colonization is probably subtle. Sat causes vacuolation of cultured bladder and kidney epithelium (11). On the other hand, it has been difficult to elucidate how Pic and Tsh contribute to the virulence of this organism.

We gratefully acknowledge J. R. Hebel, C. Drachenberg, and J. Nataro (University of Maryland School of Medicine) for contributing to the analysis of the mouse challenge experiments as well as supplying EAEC Pic and APEC Tsh proteins.

This research was supported by Public Health Service grant AI43363 from the National Institutes of Health.

REFERENCES

- Al-Hasani, K., B. Adler, K. Rajakumar, and H. Sakellaris. 2001. Distribution and structural variation of the *she* pathogenicity island in enteric bacterial pathogens. *J. Med. Microbiol.* **50**:780–786.
- Al-Hasani, K., K. Rajakumar, D. Bulach, R. Robins-Browne, B. Adler, and H. Sakellaris. 2001. Genetic organization of the *she* pathogenicity island in *Shigella flexneri* 2a. *Microb. Pathog.* **30**:1–8.
- Behren, M., J. Sheikh, and J. P. Nataro. 2002. Regulation of the overlapping *pic/set* locus in *Shigella flexneri* and enteroaggregative *Escherichia coli*. *Infect. Immun.* **70**:2915–2925.
- Datsenko, K. A., and B. L. Wanner. 2000. One-step inactivation of chromosomal genes in *Escherichia coli* K-12 using PCR products. *Proc. Natl. Acad. Sci. USA* **97**:6640–6645.
- Delicato, E. R., E. G. de Brito, A. P. Konopatzki, L. C. Gaziri, and M. C. Vidotto. 2002. Occurrence of the temperature-sensitive hemagglutinin among avian *Escherichia coli*. *Avian Dis.* **46**:713–716.
- Dutta, P. R., R. Cappello, F. Navarro-García, and J. P. Nataro. 2002. Functional comparison of serine protease autotransporters of *Enterobacteriaceae*. *Infect. Immun.* **70**:7105–7113.
- Fasano, A., F. R. Noriega, D. R. Maneval, Jr., S. Chanasongram, R. Russell, S. Guandalini, and M. M. Levine. 1995. *Shigella* enterotoxin 1: an enterotoxin of *Shigella flexneri* 2a active in rabbit small intestine in vivo and in vitro. *J. Clin. Investig.* **95**:2853–2861.
- Grodberg, J., and J. J. Dunn. 1988. *ompT* encodes the *Escherichia coli* outer membrane protease that cleaves T7 RNA polymerase during purification. *J. Bacteriol.* **170**:1245–1253.
- Guyer, D. M., J. S. Kao, and H. L. T. Mobley. 1998. Genomic analysis of a pathogenicity island in uropathogenic *Escherichia coli* CFT073: distribution of homologous sequences among isolates from patients with pyelonephritis, cystitis, and catheter-associated bacteriuria and from fecal samples. *Infect. Immun.* **66**:4411–4417.
- Guyer, D. M., I. R. Henderson, J. P. Nataro, and H. L. T. Mobley. 2000. Identification of Sat, an autotransporter toxin produced by uropathogenic *Escherichia coli*. *Infect. Immun.* **38**:53–66.
- Guyer, D. M., S. Radulovic, F. E. Jones, and H. L. T. Mobley. 2002. Sat, the secreted autotransporter toxin of uropathogenic *E. coli*, is a vacuolating cytotoxin for bladder and kidney epithelial cells. *Infect. Immun.* **70**:4539–4546.
- Henderson, I. R., J. Czczulin, C. Eslava, F. Noriega, and J. P. Nataro. 1999. Characterization of Pic, a secreted protease of *Shigella flexneri* and enteroaggregative *Escherichia coli*. *Infect. Immun.* **67**:5587–5596.
- Henderson, I. R., F. Navarro-García, and J. P. Nataro. 1998. The great escape: structure and function of the autotransporter proteins. *Trends Microbiol.* **6**:370–378.
- Johnson, D. E., C. V. Lockett, R. G. Russell, J. H. Hebel, M. D. Island, A. Stapleton, W. E. Stamm, and J. W. Warren. 1998. Comparison of *Escherichia coli* strains recovered from human cystitis and pyelonephritis infections in transurethraly challenged mice. *J. Bacteriol.* **66**:3059–3065.
- Otto, B. R., S. J. M. van Dooren, C. M. Dozois, J. Luirink, and B. Oudega. 2002. *Escherichia coli* hemoglobin protease autotransporter contributes to synergistic abscess formation and heme-dependent growth of *Bacteroides fragilis*. *Infect. Immun.* **70**:5–10.
- Otto, B. R., S. J. M. van Dooren, J. H. Nuijens, J. Luirink, and B. Oudega. 1998. Characterization of a hemoglobin protease secreted by the pathogenic *Escherichia coli* strain EB1. *J. Exp. Med.* **188**:1091–1103.
- Piva, I. C., A. L. Pereira, L. R. Ferraz, R. S. M. Silva, A. C. Vieira, J. E. Blanco, M. Blanco, J. Blanco, and L. G. Giugliano. 2003. Virulence markers of enteroaggregative *Escherichia coli* from children and adults with diarrhea in Brasília, Brazil. *J. Clin. Microbiol.* **41**:1827–1832.
- Provence, D. L., and R. Curtiss III. 1994. Isolation and characterization of a gene involved in hemagglutination by an avian pathogenic *Escherichia coli* strain. *Infect. Immun.* **62**:1369–1380.
- Rasko, D. A., J. A. Phillips, X. Li, and H. L. T. Mobley. 2001. Identification of DNA sequences from a second pathogenicity island of uropathogenic *Escherichia coli* CFT073: probes specific for uropathogenic populations. *J. Infect. Dis.* **184**:1041–1049.
- Stathopoulos, C., D. L. Provence, and R. Curtiss III. 1999. Characterization of the avian pathogenic *Escherichia coli* hemagglutinin Tsh, a member of the immunoglobulin A protease-type family of autotransporters. *Infect. Immun.* **67**:772–781.
- Tame, J. R. H., S. J. M. van Dooren, B. Oudega, and B. R. Otto. 2002. Characterization and crystallization of a novel haemoglobinase from pathogenic *Escherichia coli*. *Acta Crystallogr. D* **58**:843–845.
- Welch, R. A., V. Burland, G. Plunkett III, P. Redford, P. Roesch, D. Rasko, E. L. Buckles, S. R. Liou, A. Boutin, J. Hackett, D. Stroud, G. F. Mayhew, D. J. Rose, S. Zhou, D. C. Schwartz, N. T. Perna, H. L. Mobley, M. S. Donnenberg, and F. R. Blattner. 2002. Extensive mosaic structure revealed by the complete genome sequence of uropathogenic *Escherichia coli*. *Proc. Natl. Acad. Sci. USA* **99**:17020–17024.